A Wireless Passive Radar System for Real Time Through-Wall Movement Detection

Bo Tan, Karl Woodbridge, *Senior Member IEEE,* and Kevin Chetty

Abstract — **In this paper, a reconfigurable real time passive wireless detection system is described. The system is based on a Software Defined Radio (SDR) architecture. The signal processing method and processing flow that enable through wall target detection are introduced. The high-speed noise and interference mitigation methods implemented in the system for through wall target detection are also described. A series of experimental results are presented for both large and small human body movements in through wall scenarios. It is shown that the high resolution Doppler event history implemented in the system enables the system to recognize and distinguish between a range of body movements. The results demonstrate that this real time SDR based wireless detection system is a low cost solution for human movement and recognition with a wide range of applications.**

Index Terms—**Passive Radar, Bistatic Radar, Radar Detection, Through-Wall sensing, Gesture Detection, Wireless Communications, Software Defined Radio**

I. INTRODUCTION

The use of passive radar for non-cooperative detection is of increasing interest in many applications areas including defense, security, transport and healthcare. Passive detection uses transmitters of opportunity to illuminate the target and the increasing interest in this area is partly due to the increase in the availability of such transmitters. Research has been reported in using a wide range of transmission sources including GSM [1], DVB [2], FM [3], WiMax [4] and WiFi [5, 6]. Such systems can use single or multiple receivers and/or transmitters allowing flexible geometries to be used and adapted for different applications and scenarios. Advantages of these receive only systems include covert operation and potential ability to carry out enhanced target detection and recognition using multiple perspectives.

More recently the continually decreasing cost of high performance commercial off-the-shelf (COTS) digital components suitable for the reception and processing of these signals is also driving down the cost of passive systems well below the levels possible for good performance active radar systems. Recent passive radar hardware developments have been directed towards systems using software defined radio (SDR) architectures [7-10]. The SDR architecture is designed to relocate system functionality from hardware to software to allow a more flexible approach to radio design; conventional hardware components are instead implemented in software running on a general purpose computing device by using the digitized RF signals. SDR based passive radar can offer a number of advantages over conventional systems that includes rapid prototyping, on-the-fly reconfiguration to facilitate multiband and parameter reconfiguration operation.

Through the wall (TTW) detection has received significant attention in recent years as a result of the wide potential applications. Most TTW systems involve some form of active UWB radars [11-13]. An X-band microwave signal based through-wall detection device is claimed by GTRI in [14] called

Radar Flashlight for the purpose of sensing the small body motion by taking advantage of the high frequency RF signal. In [15], an arrival angle based through-wall detection system is reported using artificial OFDM signals. In [16], the same group of researchers have developed a 1.8 GHz bandwidth through-wall FMCW radar system which can track targets with centimeter level accuracy. In [17], a passive WiFi radar detection is described. The simulation and the experimental results show that it is possible to detect the indoor target with WiFi signal, but, the through-wall and real time capabilities are not mentioned.

Our previous paper in this area [7] utilized a full radar receiver, off line processing and had a hard wired reference source. In this paper we report on the advancements made which allow our software-defined through-wall radar to operate in real-time, and with increased Doppler sensitivity for obtaining additional target information with real WiFi signal. Unlike previous work in TTW sensing this system is able to measure both the reference and surveillance signals through walls enabling a completely stand-off and stand-alone system without any requirement to connect to an internal reference source. The hardware design and signal processing methods to enable real time high resolution Doppler performance are described. New batch data and processing techniques are introduced which facilitate very high data throughput and the detected Doppler are recorded and plotted along with the distance/time. Capability is demonstrated through a range of through wall movement experimental scenarios. Finally we describe the development of a Doppler event history which has enabled us to recognize different types of body motions. Overall the system represents a powerful and adaptable passive detection system suitable for a wide range of applications from security to healthcare.

II. SIGNAL PROCESSING AND SDR SYSTEM

To obtain target Doppler and range information, the recorded reference and surveillance channel data undergo discrete cross ambiguity function (CAF) processing (1) in LabVIEW™. For high-bandwidth signals, for example the wireless transmissions used by our system, this processing stage has a significant computational overhead which impedes real time operation.

$$CAF(\tau_d, f_d) = \sum_{n=0}^{N} r[n]s^*[n + \tau_d]e^{-j2\pi f_d \frac{n}{N}} \quad (1)$$

where N is total number of samples, n is *n-th* sample, $r[n]$ and $s[n]$ are discrete-time reference and surveillance signals in complex form, operator * is the complex conjugate of signal, τ_d is the time delay which can be converted into range information, and f_d is the Doppler shift.

To achieve real time operation without sacrificing the performance, the system employs two strategies: a pipeline processing architecture and a batch processing methodology. The batch processing permits the range-Doppler surface to be generated in a computationally efficient manner, and the

pipeline processing allows key signal and data handling procedures to be carried out simultaneously. In the following sections we describe our pipeline and batch processing approaches, and outline a DSI suppression technique which is based on the CLEAN algorithm reported previously in a through wall imaging application [18].

A. Pipeline Structure

Pipeline processing is an extension of parallel code execution that enables performance gains with serial multistage algorithms on multicore machines. A sequential code sequence is partitioned into sub-procedures which are each allocated to a separate core. The algorithm can then run simultaneously on multiple sets of recorded data, or data that streams continuously. To maximize throughput each subroutine should be carefully balanced to ensure approximately equal processing times. To optimize processing in our wireless passive radar system we divide our multistage algorithm into three subroutines: (i) reading the recorded sample data from the RAM, (ii) performing cross-ambiguity processing on this data using our batch processing technique (see Section III B) and (iii) applying our CLEAN DSI suppression algorithm (see Section III C). Fig. 1 illustrates our data pipelining strategy. As the three subroutines are implemented simultaneously, the total processing time for the system in dependent on which subroutine is taken the longest time to complete and is therefore written as (2).
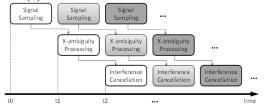

Fig. 1. Pipeline processing architecture in wireless passive radar

$$\tau_{PBR} = max\left\{\tau_{sample},\ \tau_{amb},\ \tau_{cancel}\right\} \tag{2}$$

In equation (2), τ_{sample} relies by the integration time required by system which determines its Doppler resolution, and cannot be reduced further. In order to build a real time processing flow τ_{amb} and τ_{cancel} should not be longer than τ_{sample}. In practice, interference cancellation algorithms are often simpler, thus, it is easy to control τ_{cancel} under τ_{sample}. The CAF processing requires a significant computational overhead as it involves large volumes of long sequence cross correlations and Fourier transforms. This leads to long processing times which often exceeds τ_{sample}. Batch processing is therefore introduced in the next section for fast CAF calculation.

B. Batch Processing

To reduce the processing delay τ_{amb} to less then τ_{sample} we have implemented a new batch processing method to speed up the CAF processing. The basics of batch processing are shown in Fig. 2. The method is as follows: First, the recorded synchronized reference and surveillance signals are divided into v isometric data segments respectively. Although reduced sampling potentially entails some loss of SNR, experimental results show that a 10% portion of the signal is sufficient to reliably build a clear range-Doppler surface when the signal source is active. The experiment signal source in this paper is a COTS WiFi AP which is in working status which is described

in Section IV. Secondly, the selected surveillance portion is cross-correlated with the corresponding reference portion. Then, K cross-correlation results $corr(X, Y)$ are obtained. The length of the cross-correlated sequence $corr(X, Y)$ is determined by the maximum bistatic range required in system. The cross-correlation results of each portion pair are then combined to form the matrix $\mathcal{X}_{r-d}(\tau_j, f_i)$. Finally, a Fourier transform is applied to each column of the $\mathcal{X}_{r-d}(\tau_j, f_i)$ matrix (Fig. 2). The range-Doppler surface can then be represented by the matrix $CAF(\tau, f)$. Following this DSI suppression is carried out using the CLEAN algorithm.
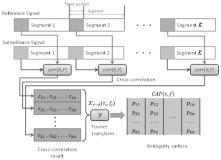

Fig. 2. Batch processing flowchart

The number of segments J is determined by the predicted maximum target velocity v_{max}. The relationship can be described by the following equation:

$$J = 2 \cdot \left\lceil \frac{v_{max}}{c} \cdot f_0 \cdot \tau_{sample} \right\rceil \tag{3}$$

where, operator $\lceil \cdot \rceil$ denotes rounding the element to the nearest integer towards infinity, c is the propagation velocity of the wireless signal, and f_0 is the centre frequency. The factor 2 is used for reserving v_{max} for both forward and backward directions.

C. Direct Signal Interference Suppression using CLEAN

After completing the above processing, the target may not necessarily be detected due to the effect of the strong direct signal interference and multipath. Thus, in this section, a simplified interference cancellation method which is modified from the CLEAN algorithm in [6] is introduced for fast computation. The purpose of the CLEAN algorithm is to mitigate the impact of the DSI and stationary clutter. These are centred on the zero-Doppler area from the original ambiguity surface $\mathcal{X}_{r-d}(\tau_j, f_i)$ obtained in Section III Part B. The impact of DSI and stationary clutter on $\mathcal{X}_{r-d}$ can be considered as the summation of a series of scaled and phased self-Ambiguity surfaces $\mathcal{X}_{r-d}^{self}(\tau_j, f_i)$ which can be calculated following the batch processing. Thus, this interference can be eliminated by subtracting the scaled and phased self-ambiguity surfaces iteratively, as shown in Eqn. (4).

$$\mathcal{X}_{r-d}^{i}(\tau_j, f_i) = \mathcal{X}_{r-d}^{i-1}(\tau_j, f_i) - \alpha_i \cdot \mathcal{X}_{r-d}^{self}\left((\tau_j - T_i), f_i\right) \tag{4}$$

where, $\mathcal{X}_{r-d}(\tau_j, f_i)$ is the resulting ambiguity surface in the i_{th} iteration, α_i is scale factor and represents the maximum value along the zero-Doppler line in $\mathcal{X}_{r-d}^{i-1}(f_i, t_j)$, T_i is the phase shift factor, determined by the time location of α_i. Generally, the calculation of (4) is much faster than the CAF processing cycle, thus, at least ten iterations can be implemented for eliminating the interference. The surface after CLEANing is denoted as $\mathcal{X}_{r-d}^{CLEAN}(\tau_j, f_i)$. In the previous tests it was found that three or four iterations are normally sufficient for clear target detection.

D. Target Detection

Using the processing methods described above a low interference range-Doppler surface can be obtained to identify target responses. We have developed a two-stage target identification routine for picking the target out from this range-Doppler surface in real time. The technique first identifies one or more areas of pixels in the range-Doppler surface display where the targets have a high likelihood of appearing. Then, a threshold is applied to assist in making a judgment on which data pixel is likely to be the target.
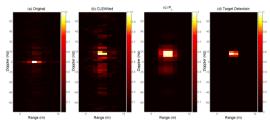

Fig. 3 Target detection processing stages from original CAF surface

Intuitively, the target is more likely to be located in an area where there are higher strength signal returns on the range-Doppler surface. But a pixel with a higher power value may not necessarily be a target since there may still be some impact from interference and clutter. A method here is introduced to highlight the most likely detection areas. The rest of the process can be described with reference to Figs. 3 and 4. The range-Doppler surfaces in Fig. 3 are based on data from a real indoor experiment carried out with the SDR wireless detection system. Fig. 3(a) is the original range-Doppler surface. The target signal is masked by the large DSI peak on the zero-Doppler line. The DSI peak is then suppressed by our modified CLEAN algorithm, forming the CLEANed surface shown in Fig. 3(b). A high intensity return pixel $p_{i,j}$ on this range-Doppler surface is then chosen. This pixel and its neighboring pixels are defined as sub-surface $\mathcal{X}_{r-d}^{i,j}$ (Fig. 4(a)).
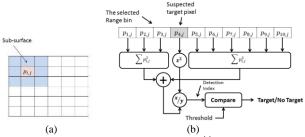

Fig . 4 (a). Definition of the sub-surface $\mathcal{X}_{r-d}^{i,j}$, (b). Modified cell

We can then further refine the areas of highest power return using equation (5).

$$P_{i,j} = \sum_{i-1,j-1}^{i+1,j+1} p_{i,j}^2 \tag{5}$$

Then, a new range-Doppler surface $\mathcal{X}_{susp}$ showing only the areas with high likelihood of target detection can be obtained (Fig. 3 (c)). Following these range bins containing the high intensity returns remaining on the CLEANed surface $\mathcal{X}_{r-d}^{CLEAN}$ are picked and analyzed with a cell averaging algorithm for making a judgment on whether a target is present. The cell averaging method is illustrated in Fig. 4 (b). The detection index defined in Fig. 4 (b) is the ratio of P_{ij} to the sum energy of all the other pixels in the selected range bin. We define this

index as the event intensity index $I_{i,j}$:

$$I_{i,j} = \frac{p_{i,j}^2}{\sum_{k \neq i} p_{k,j}^2} \tag{6}$$

Once the target/no-target decision is made the final confirmed target detection is displayed as illustrated in Fig. 3(d).

E. Information Display

The detection index $I_{i,j}$ can be used for indicating how significant in terms of effective signal return above background the detected event is. Clearly, a target which has a large cross section will generate a larger detection index, than a smaller less conspicuous target. Once a target is detected, the system can make a record of the detection. Our real time system will output the Doppler record continuously. By using this record, time-Doppler characteristics can be obtained and displayed. This Doppler event history gives a very clear view of target movement status varying with time and can be used to characterize a range of movements.
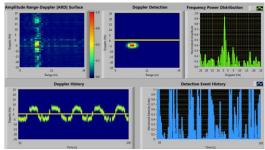

Fig. 5. Graphic system display

Following on the above processing a user display has been developed to give a clear visual record of the detected events (Fig. 5). The real time information that can then be displayed for inspection is; raw range-Doppler surface (top left), processed and CLEANed target detection in range and Doppler (top middle), frequency spectrum of the range bin which contains the target (top right), Doppler history (bottom left) and detection event intensity (bottom right). This display thus gives a comprehensive summary of target detection events and characteristics enabling wide range information to be deduced. It should be noted that the detection will be displayed with time lag after the event taking place due to the sampling duration needed for the CAF processing. In the walking/running scenario the sampling duration is set to 0.5 sec. This means the Doppler display lags 0.5 sec behind the actual movement. For the body gesture detection a longer sampling duration is used for higher Doppler resolution, meanwhile a step shift method [19] is used to reduce the time lag to approximately 25 ms.

F. Software defined radio system

A complete SDR passive detection system consists basically of antennas, up/down converters, an ADC/DAC and some form of computing unit. Usually the up/down converter and ADC/DAC functions are integrated into one module. The computing unit can be any reconfigurable computing platform with an operating system which can implement high speed signal processing software. Thus, the computing unit can be a PC or embedded chip with its own inbuilt operating system. The overall architecture of the SDR wireless passive radar is shown in Fig. 6. The main design considerations for the system are briefly described in the following sections. The signal

processing architectural and method described in Section II *A* to *F* are implemented in the computing unit in Fig. 6.
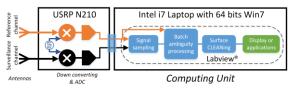

Fig 6. Block diagram of software defined passive wireless system

III. EXPERIMENTS AND RESULTS

A series of experiments have been carried out to test the capability of the real time SDR passive WiFi detection system. In the following experiments RocketDish RD-2G24 dish antennas were used for the reference and surveillance channels. These operate over a range of 2.3 ~ 2.7 GHz with 24 dBi gain and a narrow beam width of 3.8˚. The Ettus Universal Software Radio Peripheral (USRP) N210 is used for RF down-conversion, ADC and digitising with the reference and surveillance channels synchronized by a MIMO cable. The data processing unit is a laptop equipped with an Intel Core i7-3940XM 3.2 GHz CPU and 64 bits Windows7. The operating system provides multiple threads option to implement our pipeline processing (Fig. 1) in the LabVIEW™ software platform used.

A. Experiment Setup and Scenarios

A first series of experiments was carried out to investigate the ability of the system to detect a human target obscured by a wall. An equipment storage building located in a sports field was used as the test site. The scenario used for the experiments is shown in Fig. 7. The test venue is built with a brick/block wall and metal roof. The thickness of the wall is 30 cm. The WiFi access point used in experiment was an Edimax Wireless 3000M with 15 dBm transmission power. To replicate many typical WiFi installations the AP was mounted on the inside of the wall. The WiFi AP in experiment is in active status while two laptops are communicating via the AP. The reference antenna and surveillance antenna were placed outside the building and were separated by 1.5 m. The reference antenna was positioned to point in the general direction of the WiFi AP in order to optimize the reference signal, while the surveillance antenna was directed towards the general target test area within the building. Two different experimental scenarios were designed for assessing the capabilities of the system. 1). through wall personnel detection, and 2). human body movements by using real time high resolution Doppler history data.
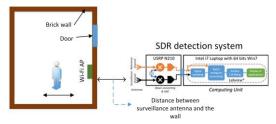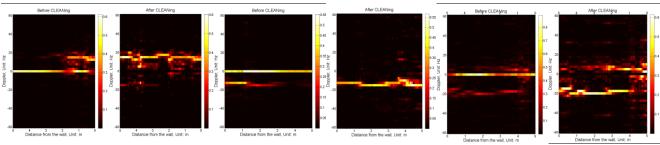

Fig. 7. The experimental scenario, data acquisition and processing system

B. Through the Wall Personnel Detection

For the walking person scenario, the integration time is set to 0.5 seconds, giving a 2Hz Doppler resolution. In most previous research such as [5, 6] the reference signal is obtained by tapping off the signal directly from the WiFi AP. This is however not feasible or desirable in practical applications. Thus, in this work the through-wall in-air reference signal is used with a reference antenna outside the wall at a distance of 1.5 meters. This mode of operation makes it possible to deploy the system as a stand-alone sensor set up inside or outside of the target building and much closer to a realistic deployment. In this section, we describe three different experimental scenarios which were designed to fully test the TTW capability of the system: **1).** Single targets moving in opposite directions, **2).** Two targets moving in opposite directions and different velocities, **3).** Repeat of the single target experiment with increasing stand-off distances between the surveillance antenna and the wall.

Single Target Experiments: This experiment consisted of a single person walking towards and away from the wall at a constant velocity. The target movement was in the range of approximately 5m in side of the wall in the geometry shown in Fig. 8 (a, b). The Doppler detection as a function of range from the wall both before and after the CLEAN algorithm is applied is shown in Fig 8 (a, b). Prior to application of CLEAN, the target returns in both forward and backward directions is visible up until the target is around 2 m from the wall. After that the return is masked by the zero-Doppler returns from DSI, the wall and other stationary objects. After CLEANing the data, the target can clearly be identified at a negative or positive Doppler of around 18 Hz throughout the walking range for movements in both directions. This corresponds to a walking velocity of approximately 2.2 ms^{-1} which is consistent with the target walking speed. Notice that the detected Doppler intensity shown in Fig. 8 are displayed in normalized with respect to maximum value on immediate CAF surface not the absolute power level as we are interested the contrast between background and signal for detection purpose. The normalized

(a). Walking person approaching the wall   (b). Walking person leaving the wall   (c). Two walking targets

Fig. 8. Doppler records for a single target moving (a, b) and two targets in opposite moving directions (c)

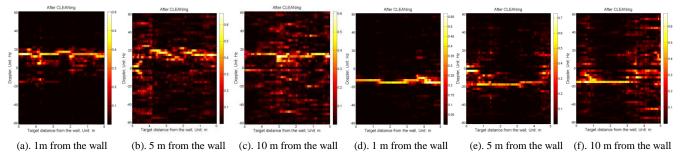| (a). 1m from the wall | (b). 5 m from the wall | (c). 10 m from the wall | (d). 1 m from the wall | (e). 5 m from the wall | (f). 10 m from the wall |

Fig.9. Doppler records for a single target approaching (a, b, c)/leaving (d, e, f) the wall with different surveillance antenna stand off distances.

scale is applied in the similar style for presenting the Doppler detection intensity in the following figures.

Two Targets Experiments: The objective was to demonstrate the capability of the system to distinguish targets in close proximity using Doppler only. In this experiment one person walks away from the wall with a fixed speed while another person walks towards the wall with a fixed but lower speed than the first person. The results are shown in Fig. 8 (c). Prior to application of CLEAN the zero-Doppler and DSI cause considerable masking of the target signals although some detection of the faster target is apparent. After CLEANing the two clear traces are seen at the expected Doppler shift areas. It is noticeable that the data is much noisier in the ranges close to and far from the wall. We believe this is due to two factors: masking of the far target signal by the closer person and dynamic multipath. There is also a fact related to the increasingly different ranges of the targets in these positions resulting in an increasing difference in signal return strength as the targets reach the end walking range. Despite these limitations the two targets can clearly be distinguished in throughout the range even when in close proximity at 2.5m when they pass each other. The difference in walking speed is also clearly seen.

Varying Surveillance Stand-off Distance: In this experiment, the surveillance antenna was positioned at stand-off distances of 1, 5 and 10m away from the wall. In each case the surveillance antenna was moved back in a line perpendicular to the wall so the pointing direction remained the same. Recorded Doppler data corresponding to these distances are shown for a person approaching (Fig. 9 (a, b, c)) and leaving (Fig. 9 (d, e, f)) the wall. Doppler is clearly seen even at the 10 m stand-off distance and with the target some 5 m from the wall after CLEAN algorithm. The 10 m stand-off result shows increased noise due to degrading signal to noise ratio as a result of the greater range and also increasing interference from returns in the expanding surveillance area as the antenna is moved farther away from the wall. Overall these results represent a significant achievement showing detection of a moving person through wall at comparable long surveillance to target range.

C. Through Wall Gesture Detection and Results

The experiments in Section B demonstrated the capability of the system to detect significant whole body displacement, but for the body gesture, it may contain different velocity components, for example the leg, arm or torso, move within a relatively large dynamic speed range. This is usually of the order of 0.25 m/sec to 4 m/sec which will cause 3.8 Hz to 64 Hz Doppler shifts. This large dynamic range requires higher Doppler resolution. Thus, a longer integration time is used in this experiment. For the relatively small and/or slow body movements to be measured in these experiments we used virtually 5 second integration time which is equivalent to 0.2 Hz Doppler resolution. This experiment was carried out with the same antennas and similar geometry as previously shown in Fig. 7, but in an indoor office environment with a 22 cm thickness wall, and the reference and surveillance antennas were located outside the wall of the experimental surveillance area at distances of 1 and 1.5 m respectively. In general, the wall will result in electromagnetic effect on the WiFi signal. In this paper the wall attenuation is used for indicating the simplified the EM effect of the wall. The attenuation of the brick wall is measured in [15] and [20].

For the purpose of capturing details of the movement, a 25 ms step shift is applied between successive integrations. In this experiment four body gestures, back-forward swing (Fig. 10(d)), left-right swing (Fig. 10(b)), squatting-standing (Fig. 10 (c)) and stooping (Fig. 10 (d)), were measured. The dynamic Doppler shift range is ±10 Hz. These TTW gesture results show clear differences distinctive characteristics between each movement. There is significant detail to be analyzed in this date and this investigation is on-going. In this paper we report some preliminary observations on these results.

Stooping: During this gesture cycle, only the upper body is moving and approaching or leaving the antenna. Thus, predictably a positive and negative Doppler is generated. The stoop – stand sequence is normally completed quickly as it is a difficult motion to perform slowly. Thus, the Doppler record shows a much sharper characteristic than in the other motions. In addition, the detected signal strengthen is not as strong due to the more limited span of the body movement. Fig. 10 (b) clearly shows these Doppler record characteristics.

Left-right swing: In this experiment the subject was facing the wall pointing towards the surveillance antenna on the other side and swinging the torso from left to right. In this geometry the torso movement is angled rather more obliquely towards the bistatic baseline giving slightly smaller bistatic Doppler than the above case and movement occurs in a double cycle. This results in initially positive Doppler followed by significant negative Doppler trough as the torso swings through the complete return cycle. This is then followed by positive Doppler again as the torso swings upright. (Fig. 10(c)).

Squatting-standing: During the squatting-standing gesture cycle, the situation becomes more complex since different parts of the body may have different motions. For example, when squatting down, the knee is moving forward, while the waist is
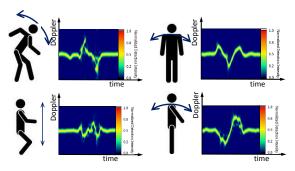
Fig. 10. Through Wall Body Movement Real Time Doppler Records, (a) stooping, (b) left-right swing, (c) squatting-standing, (d) back-forward swing.

moving backward, meanwhile upper body has slight forward lean. A reverse procedure will occur during the standing period. The Doppler record (Fig. 10(c)) of this gesture cycle shows a combination of positive and negative excursions.

Back-forward swing: In this case the upper torso swings directly towards or away from the surveillance antenna at a slight angle to the bistatic baseline. This results in a characteristic sinusoidal positive and negative Doppler which is clearly visible in the Doppler record in Fig. 10 (d). As mentioned previously, there is a great deal of information that can be extracted from these characteristics. This includes number, type and magnitude of Doppler events, event sequence and Doppler/time characteristics of each event. These characteristics are also suitable for classification using micro-Doppler methods we have used in previous active radar research [21]. These features can potentially give detailed information on the characteristics of many types of movements.

IV. CONCLUSIONS

In this paper we have reported on the development of a real time through wall WiFi passive radar system. The software defined hardware architecture and high speed signal processing are described. We demonstrate that using a pipelined batch processing technique we can achieve close to real time operation despite the very high cross-correlation data rate. We also describe the DSI and interference methods used to enable target detection in high clutter and multipath environments. A new algorithm for highly effective target detection confirmation on the time-Doppler record is also introduced. The system capability is demonstrated in a series of through-wall experiments. These experiments were carried our without a tapped off reference as in many previous reports on through-wall detection and used external stand-off surveillance and reference receivers. Despite this challenging environment we have shown that moving single and multiple targets can be detect at surveillance receiver distances up to 10 m through substantial brick/block walls. A method for displaying the Doppler event history is also presented and shown to be a very useful means of identifying movement characteristics. Preliminary characterization of some different movements show a range of interesting features which can potentially be used to classify various actions even through the wall. Reference [21] describes Doppler characteristics extraction and classification method in the bistatic scenario. For our work, the typical gestures in specific scenarios, for example healthcare, security and human machine interaction (HCI), will be selected as follow-up of this paper. To approach applications scenarios,

machine learning methods will be introduced to interpret the passive radar detection results. Our real time detection system will inspire series of cross disciplinary and applications researches.

REFERENCES

[1] Krysik, P, Samczynski, P., Malanowski. M., Maslikowski, L. and Kulpa, K.S., "Velocity measurement and traffic monitoring using a GSM passive radar demonstrator", in *IEEE Aerosp. and Electron. Syst. Mag.*, vol.27, no.10, pp.43-51, 2012.

[2] Palmer, J.E., Harms, H.A., Searle, S.J. and Davis, M.L., "DVB-T passive radar signal processing", in *IEEE Trans. Signal Process.*, vol.61, no.8, pp.2116-2126, 2013.

[3] Brown, J., Woodbridge, K., Stove A. and Watts, S., "Air target detection using airborne passive bistatic radar", in *IEEE Lett. Electron..*, pp.1396-1397, 2010.

[4] Chetty, K., Woodbridge, K., Guo, H. and Smith, G.E., "Passive bistatic WiMAX radar for marine surveillance," in *2010 IEEE Radar Conference*, pp.188-193, Washington, DC, May, 2010.

[5] Falcone, P., Colone, F., Macera, A. and Lombardo, P., "Two-dimensional location of moving targets within local areas using WiFi-based multistatic passive radar," in *IET Radar, Sonar & Navigation*, vol.8, no.2, pp.123,131, February 2014.

[6] Chetty, K., Smith, G.E. and Woodbridge, K., "Through-the-wall sensing of personnel using passive bistatic WiFi radar at standoff distances", in *IET Trans. Geosci. Remote Sens.*, vol.50, no.4, p. 1218-1226, 2012.

[7] Woodbridge, K., Chetty, K., Young, L., Harley, N. and Woodward, G., "Development and demonstration of software- radio-based wireless passive radar", in *IET Lett Electron.*, vol.48 no.2, pp. 120-121, 2012.

[8] Jamil, K., Alhekail, Z.O. and Al-Humaidi, S., "A multi-band multi-beam software-defined passive radar part II: Signal Processing", in *2012 IET International Conference on Radar*, pp. 1-5. Glasgow, UK, Nov. 2012.

[9] Heunis, S., Paichard, Y. and Inggs, M., "Passive radar using a software-defined radio platform and open source software tools", in *2011 IEEE Radar Conference*, pp. 879-884, Kansas City MO, May. 2011.

[10] Berizzi, F., Martorella, M., Petri, D., Conti, M. and Caprcia, A., "USRP technology for multiband passive radar", in *2010 IEEE Radar Conference*, pp. 225-229, Washington, DC, May. 2010.

[11] Gomez, J. A. and Brooker, G., "A Ultra-Wideband radars for through-wall imaging in robotics," in *Recent Advances in Sensing Technology*, pp. 271-282. 2009.

[12] Fontana, R.J., "Recent system applications of short-pulse ultra-wideband (UWB) technology," in *IEEE Transactions on Microwave Theory and Techniques*, vol. 52, pp. 2087-2104, 2004.

[13] Sisma, O., Gaugue, A., Liebe, C. and Ogier, J., "UWB radar: vision through a wall," in *Telecommunication Systems*, vol. 38, pp. 53-59, 2008.

[14] Hunt, A., Tillery, C. and Wild, N., "Through-the-wall surveillance technologies" in *American Correctional Association, Correction Today*, vol. 63, No. 4, Jul, 2001.

[15] Adib, F. and Katabi, D., "See through walls with Wi-Fi", in *ACM Special Interest Group on Data Communication*, Hong Kong, Aug. 2013.

[16] Adib, F., Kabelac, Z., Katabi, D. and Miller, R.C., "3D tracking via body radio reflections", in Proceedings of the *11th USENIX Symposium on Networked Systems Design and Implementation (NSDI '14),* Seattle, WA, Apr. *2014*.

[17] Buonanno, A., D'Urso, M. and Palmieri, L., "WiFi-based passive bistatic radar by using moving target indicator and least square adaptive filtering," in *IEEE International Symposium on Phased Array Systems & Technology*, Waltham, Massachusetts, Oct. 2013

[18] Chang, P.C., Burkholder, R.J. and Volakis, J.L., "Adaptive CLEAN with target refocusing for through-wall image improvement," in *IEEE Transactions on Antennas and Propagation*, vol. 58, pp. 155-162, 2010.

[19] Balleri, A., Woodbridge, K. and Chetty, K., "Frequency-agile non-coherent ultrasound radar for collection of micro-Doppler signatures," in *2011 IEEE Radar Conference*, pp.045-048, Kansas City, MO, USA, May 2011.

[20] Ogunjemilua, K., Davies, J.N., Grout, V. and Picking, R., "An investigation into signal strength of 802.11n WLAN," in *Fifth Collaborative Research Symposium on Security, E-Learning, Internet and Networking*, pp.26-27, Darmstadt, Germany, Nov. 2009.

[21] Smith, G.E., Woodbridge, K., Baker, C.J. and Griffiths, H., "Multistatic micro-Doppler radar signatures of personnel targets", in *IET Sig. Proc.*, vol.4, no.3, pp.224-233, 2010.

Bo Tan received the B.S. degrees in communications engineering in 2004 and M.Sc. degree in circuit and system 2008 from the Beijing University of Posts and Telecommunications, Beijing, China. He obtained the Ph.D. degree in Digital Communications from the University of Edinburgh, UK, in 2013. He is currently a research associate with the Department of Computer Science, and honorary senior research associate with the Department of Electronic and Electrical Engineering, University College London. His research includes signal processing methods and system design and application development for wireless based passive radar and array processing and wireless sensor network.

Karl Woodbridge (SM '12) is Professor of Electronic Engineering in the Sensor Systems and Circuits group at University College London. Current RF research activities at UCL include multi-static and netted radar systems, sea clutter, target tracking and classification and land and air based passive sensing. His research activities have been carried out in research investigator and technical consultancy roles for a wide range of customers in the civil and defense areas. He has published or presented over 200 journal and conference papers and has served on organizing and technical committees for many national and international conferences. He is a Senior Member of the IEEE, Fellow of the IET and a Fellow of the UK Institute of Physics.

Kevin Chetty (M'05) received the B.Phys. degree and the M.Sc. degree in X-ray physics from King's College London, London, U.K., in 2003 and the Ph.D. degree in modeling and advanced detection strategies for ultrasound contrast agents from Imperial College London, London, in 2007. He is currently a Lecturer with the Department of Security and Crime Science, University College London, London. His research focuses on new passive RF sensor systems that exploit transmitters of opportunity for uncooperative detection of personnel, vehicle, and marine targets. Other research interests include target detection and classification using acoustic micro-Doppler signatures, through-the-wall radar, and software-defined sensor systems. He is a reviewer for the IET Radar, Sonar, and Navigation journal. Dr. Chetty is a member of the Institution of Engineering and Technology